Materials and Design 103 (2016) 71–74

Contents lists available at ScienceDirect

Materials and Design

journal homepage: www.elsevier.com/locate/matdes

Mechanism of magnetic transition in FeCrCoNi-based high entropy alloys

Shuo Huang [a,*], Wei Li [a], Xiaoqing Li [a], Stephan Schönecker [a], Lars Bergqvist [b], Erik Holmström [c], Lajos Károly Varga [d], Levente Vitos [a,d,e,**]

[a] Applied Materials Physics, Department of Materials Science and Engineering, Royal Institute of Technology, Stockholm SE-100 44, Sweden
[b] Department of Materials and Nano Physics, Royal Institute of Technology, Electrum 229, SE-16440 Kista, Sweden
[c] Sandvik Coromant R&D, 126 80, Stockholm, Sweden
[d] Institute for Solid State Physics and Optics, Wigner Research Centre for Physics, H-1525 Budapest, P.O. Box 49, Hungary
[e] Department of Physics and Astronomy, Division of Materials Theory, Uppsala University, Box 516, SE-75120 Uppsala, Sweden

ARTICLE INFO

Article history:
Received 8 January 2016
Received in revised form 15 April 2016
Accepted 17 April 2016
Available online 20 April 2016

Keywords:
High-entropy alloy
Magnetic transition
Monte-Carlo simulation
First-principles calculation

ABSTRACT

First-principles alloy theory and Monte-Carlo simulations are performed to investigate the magnetic properties of $FeCrCoNiAl_x$ high entropy alloys. Results show that face-centered-cubic (fcc) and body-centered-cubic (bcc) structures possess significantly different magnetic behaviors uncovering that the alloy's Curie temperature is controlled by the stability of the Al-induced single phase or fcc-bcc dual-phase. We show that the appearance of the bcc phase with increasing Al content brings about the observed transition from the paramagnetic state for FeCrCoNi to the ferromagnetic state for FeCrCoNiAl at room-temperature. Similar mechanism is predicted to give rise to room-temperature ferromagnetism in FeCrCoNiGa high entropy alloy.

1. Introduction

The newly developed high-entropy alloys (HEAs) represent one of the most promising fields of metallurgy and open an exciting research area in condensed matter physics [1–3]. These alloys usually consist of four or more elements with equal or nearly equal concentrations and form simple solid solution phases often with face-centered cubic (fcc) and body-centered cubic (bcc) structures. Among the most common HEAs, the FeCrCoNi-based alloys attracted much attention due to the great variety of interesting and unusual properties [4–15]. For example, recent magnetization measurements indicated that the addition of Al causes the magnetic state of equimolar alloy FeCrCoNi to change gradually from paramagnetic to ferromagnetic at room temperature [9–11]. The mechanism behind the Al-induced magnetic ordering is of particular interest due to the fact that Al is a non-magnetic metal, and opens the possibility to design and optimize magnetic materials based on HEAs in the future. So far, very few investigations devoted to this question have been presented, which may be attributed to the complexity of the problem related to the chemical and magnetic disorder present in HEAs. In the present letter, we put forward a comprehensive study of the magnetic properties for $FeCrCoNiAl_x$ HEAs by using first-principles quantum mechanical methods and classical Heisenberg Monte-Carlo (MC) simulations.

2. Theoretical methods

The magnetic properties can be described using the effective Heisenberg-like Hamiltonian, $H = -\sum_{i,j} J_{ij}\mathbf{m}_i \cdot \mathbf{m}_j$, where J_{ij} denotes the strength of magnetic exchange interaction between atomic sites i and j with magnetic moments $\mathbf{m}_i$ and $\mathbf{m}_j$. The parameters of the above Hamiltonian can be determined from *ab initio* calculations employing the magnetic force theorem in the ferromagnetic state [16]. Here, we adopted the exact muffin-tin orbitals (EMTO) method [17,18] in combination with the coherent potential approximation (CPA) [19,20] to compute the J_{ij} parameters of HEAs (in ferromagnetic state) as a function of chemical composition and crystal structure. The exchange-correlation effects were treated within the generalized gradient approximation (GGA) in the form of Perdew-Burke-Ernzerhof (PBE) [21,22]. The calculations were performed within the scalar relativistic approximation and soft-core scheme. The muffin-tin basis set included *s*, *p*, *d* and *f* orbitals. The electrostatic correction to the single-site CPA was described using the screened impurity model with screening parameter 0.6 [23].

3. Results and discussion

In Fig. 1 we present the calculated Wigner-Seitz radius for the $FeCrCoNiAl_x$ ($0 \le x \le 2$) HEAs. Here, the fcc phase is considered for

* Corresponding author.
** Corresponding author at: Applied Materials Physics, Department of Materials Science and Engineering, Royal Institute of Technology, Stockholm SE-100 44, Sweden.
E-mail addresses: shuoh@kth.se (S. Huang), levente@kth.se (L. Vitos).

http://dx.doi.org/10.1016/j.matdes.2016.04.053
0264-1275/

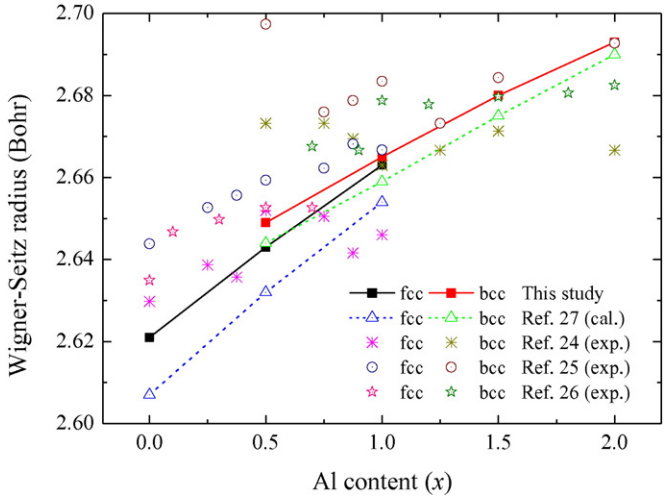

Fig. 1. Comparison between the theoretical and experimental Wigner–Seitz radii of fcc and bcc $FeCrCoNiAl_x$ alloys. The references for the previous theoretical and experimental studies are indicated in the legend.

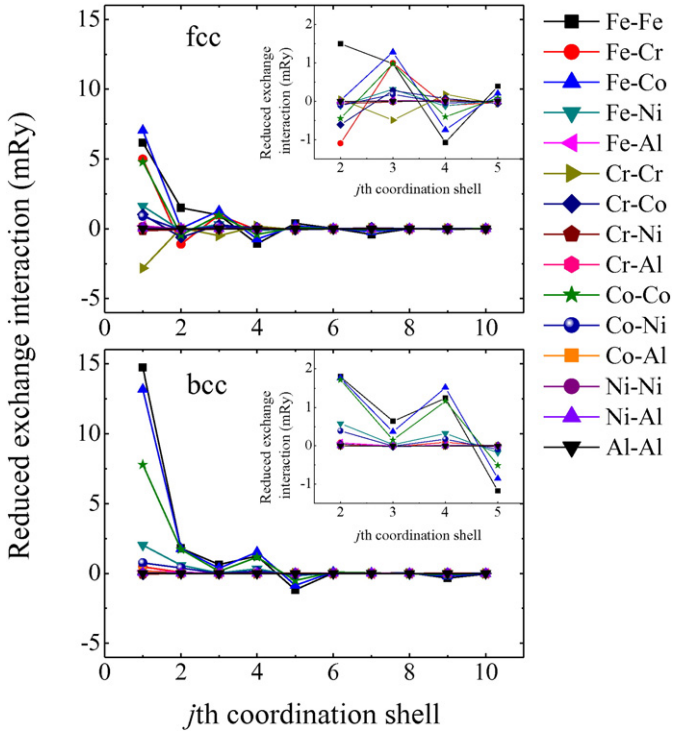

Fig. 2. Magnetic exchange interactions for equiatomic FeCrCoNiAl as a function of the coordination shell for fcc and bcc phases, respectively.

$x \le 1$ and the bcc one for $x \ge 0.5$ according to microstructure observations [11,24–26] and previous theoretical prediction [27]. Despite the large scatter in the experimental data, the present theoretical work reproduces the experimental trend, that Al additions increase the volume of the solid solution. The magnetic moments of the systems at corresponding volumes are summarized in Table 1. It is found that, in both fcc and bcc phases, the non-magnetic alloying element Al is nearly non-polarized (or slightly anti-parallel with Fe/Co/Ni). Further analysis shows that both the Al concentration and the crystal structure play important role in the change of magnetic moments for the present alloys. For example, the magnetic moment per Co atom decreases from 1.12 μ_B at $x = 0$ to 0.97μ_B at $x = 1$ in the fcc phase, whereas in the bcc phase it varies from 1.44 μ_B to 1.19 μ_B when x changes from 0.5 to 2. The total magnetic moment per atom for FeCrCoNiAl in the bcc phase is 0.74 μ_B, which is 48% larger than the one in the fcc phase. In both phases, Al addition is found to decrease the total magnetic moments, which is consistent with the fact that Al is a non-magnetic metal.

Further insight into the magnetic properties of alloys can be obtained by considering the magnetic exchange interactions between alloy components. Here, a reduced exchange interaction parameter $J_{ij}^{'} = z_p J_{ij} \boldsymbol{m}_i \cdot \boldsymbol{m}_j$, where z_p is the coordination number of the pth coordination shell, is employed to better understand the crystal structural effects. The obtained results for FeCrCoNiAl HEA in zero magnetic field are shown in Fig. 2. It is found that the interactions show long-range oscillatory behavior, e.g., the Fe–Fe interaction is predominantly ferromagnetic but may have anti-ferromagnetic contributions depending on the distance between the Fe atoms. Further analysis shows that the ferromagnetic interactions in the fcc phase are mainly from the nearest-neighbor Fe–Fe, Fe–Co, and Co–Co pairs, and the anti-ferromagnetic interactions between Fe–Cr and Cr–Cr pairs. Notice that the positive value of the exchange parameter between Fe and Cr reflects an anti-ferromagnetic coupling due to the fact that the Cr magnetic moment is anti-parallel to that of Fe (as shown in Table 1). In the case of the bcc phase, the anti-ferromagnetic couplings between Fe–Cr and Cr–Cr at the nearest-neighbor distance are small and negligible. In addition, the dominating ferromagnetic interactions (Fe–Fe, Fe–Co and Co–Co pairs at the nearest-neighbor shell) in the bcc phase are much stronger than those in the fcc phase. These features demonstrate that the crystal structure has a strong impact on the ferromagnetic behavior of FeCrCoNiAl.

Table 1
Theoretical total and partial magnetic moments (units of μ_B per atom) for $FeCrCoNiAl_x$ high entropy alloys in both fcc and bcc phases as a function of Al fraction x.

	fcc			bcc			
	$x = 0$	$x = 0.5$	$x = 1$	$x = 0.5$	$x = 1$	$x = 1.5$	$x = 2$
Fe	1.96	1.97	1.98	2.23	2.17	2.13	2.08
Cr	−0.72	−0.64	−0.60	−0.09	−0.07	−0.05	−0.03
Co	1.12	1.04	0.97	1.44	1.34	1.26	1.19
Ni	0.30	0.23	0.19	0.31	0.27	0.24	0.21
Al	–	−0.05	−0.04	−0.03	−0.03	−0.03	−0.03
Total	0.66	0.57	0.50	0.86	0.74	0.64	0.57

Starting from the computed magnetic exchange interactions, we performed MC simulations using the UppASD program [28] to estimate the Curie temperature of $FeCrCoNiAl_x$ HEAs as a function of Al content and crystal structure. This approach has previously been successfully applied to a large number of metallic systems [29–31]. The MC simulation boxes contained up to 108,000 atoms (subject to periodic boundary conditions) for the fcc crystal lattice and up to 128,000 atoms for the bcc one. Random distributions of alloy components in the supercells were generated for the studied HEAs, and 20,000 MC steps have been used for equilibration followed then by 20,000 steps for obtaining thermodynamic averages. Fig. 3a shows the obtained normalized magnetization (M/M_0, with M and M_0 being the magnetization at T and 0 K, respectively) as a function of temperature for FeCrCoNiAl. The effect of the crystal structure can be clearly observed, namely, the magnetic transition temperature in the bcc phase is much higher than that in the fcc phase. To estimate the critical temperature, in Fig. 3b we present the temperature dependence of the magnetic susceptibility ($\chi = [\langle M^2 \rangle - \langle M \rangle^2]/k_B T$) obtained from the MC calculations with varying system sizes. Notice that χ diverges at the critical temperature in the thermodynamic limit in the absence of an external magnetic field. From the robust susceptibility peak, we find that the Curie temperature for the FeCrCoNiAl HEA is 205 ± 5 K for the fcc phase and 355 ± 5 K for the bcc phase.

Applying the above procedure to fcc and bcc $FeCrCoNiAl_x$ alloys with various x values, we obtained the concentration dependence of the theoretical Curie temperature for both phases. The present results are compared with the available experimental values [11] in Fig. 4. It is clear that the Curie temperature of the current HEAs is strongly dependent on the